CONIN H2020-MSCA-RISE-2016

Action acronym: CONIN

Action full title: Effects of confinement on inhomogeneous systems

Grant agreement No 734276

Work Package 1

Modelling of self-assembly in systems with competing interactions (Months: 1-48)

Task 1.3

Effects of confinement on self-assembling systems the case of simple geometry of confining walls (Months:25-36)

Deliverable D1.3

Structural, thermodynamic and mechanical properties of confined systems with SALR interaction

In 2019 the planned task was:

Task 1.3 **Effects of confinement on self-assembling systems - the case of simple geometry of confining walls**

"Numerical simulations will be implemented to study the structures and behaviours of self-assembling systems confined in various simple geometries. Monte Carlo, mainly, and also molecular dynamics are the numerical techniques to be applied. The interacting particles can be confined by the walls, or the walls can be the support of the particles (e.g., nanoparticles on the surface of a sphere). The confining walls (rigid or elastic, permeable or impervious) could determine a spherical volume, a cylindrical tube, a slit pore (parallel walls), a symmetrical or asymmetrical dumbbell volume (two intersecting spherical volumes), or simply a two dimensional stripe. Though the efforts will be focused in the structure and pattern formation, in particular systems also the dynamics of the aggregation could be studied. Lead Participant: UNLP (G. Zarragoicoechea) UNLP, BSTU, CSIC, IPC will perform simulation studies for different models, compare and interpret the results."

The activities in WP1 in 2019 were the following:

1. **Effect of self-assembly on structural and thermodynamic properties near a confining wall.**
    a. Effect of aggregation on adsorption phenomena.
    b. Adsorption anomalies in a 2D model of cluster-forming systems.
    c. Soft-particle fluid with competing interactions confined by a hard wall.
    d. Adsorption of SALR particles on spherical surface.
    e. Mesoscopic theory for systems with competing interactions near a confining wall.
    f. Microscopic theory for non-homogeneous systems with competing interactions.
2. **Core-shell particles self-assembling on an interface between coexisting fluid phases.**
3. **Simulation studies of the SALR systems under confinement.**
    a. SALR confined in pipes of different cross-sections.

b. SALR confined in spherical shells.

4. **Hyperuniformity in systems with competing interactions.**

   a. Hyperuniformity and structure of dipolar fluids on curved surfaces.

   b. Extension to other curved surfaces.

   c. A minimal model for avian retina.

1. Effect of self-assembly on structural and thermodynamic properties near a confining wall

1.a. Effect of aggregation on adsorption phenomena. Adsorption at an attractive surface in a system with particles self-assembling into small clusters was studied by Molecular dynamics (MD) simulation. We assumed the short-range attraction long-range repulsion (SALR) potential that consists of Lennard-Jones plus repulsive Yukawa tail,

$$u(r) = 6\epsilon\left[\left(\frac{\sigma}{r}\right)^{12} - \left(\frac{\sigma}{r}\right)^{6}\right] + \frac{A}{r}e^{-r/\xi}, \tag{1}$$

where ϵ and σ set the energy and length units, $A = 1.8$ and $\xi = 2$. The dimensionless temperature is defined as $T^* = k_B T/\epsilon$, where k_B is the Boltzmann constant. We focused on small densities.

In the first step, structural and thermal properties of the bulk were investigated. We determined critical cluster concentration (CCC). At the CCC, a peak in the histogram of the cluster size distribution appears for a particular number of particles. The CCC is similar to the critical micelle concentration. In addition, we discovered a new structural crossover between monomer- and cluster-dominated fluid. At this crossover: (i) the probability of finding an isolated particle is equal to the probability of finding a particle belonging to the cluster of the optimal size (ii) the histogram of the cluster size distribution has two maxima of equal hight and (iii) the specific heat takes a maximum.

For the wall-particle interactions we assumed

$$V_L(z) = \gamma\epsilon\left[\left(\frac{\sigma}{z - z_L}\right)^{12} - \left(\frac{\sigma}{z - z_L}\right)^{6}\right]. \tag{2}$$

The relative increase of the temperature at the critical cluster concentration near the attractive surface (CCCS) shows a power-law dependence on the strength of the wall-particle attraction. At temperatures below the CCCS, the adsorbed layer consists of undeformed clusters if the wall-particle attraction is not too strong. Above the CCCS, or for strong attraction leading to flattening of the adsorbed aggregates, we obtain a monolayer that for strong or very strong attraction consists of flattened clusters or stripes respectively (Fig.1). The accumulated repulsion from the particles adsorbed at the wall leads to a repulsive barrier that slows down the adsorption process, and the accession time grows rapidly with the

strength of the wall-particle attraction. Beyond the adsorbed layer of particles, a depletion region of a thickness comparable with the range of the repulsive tail of interactions occurs, and the density in this region decreases with increasing strength of the wall-particle attraction (Fig.2b). Thus, the attractive surface becomes effectively repulsive when it is covered by a layer of particles that repell one another at large distances. At larger separations, the exponentially damped oscillations of density agree with theoretical predictions for self-assembling systems,

$$g(z) := \rho(z)/\rho_g = 1 + A\sin(\alpha_1 r + \phi)e^{-\alpha_0 r}, \tag{3}$$

where ρ_g is the density far from the wall. α_1 and α_0 take the same values as for the pair distribution function in the bulk at the same thermodynamic conditions (Fig.2).

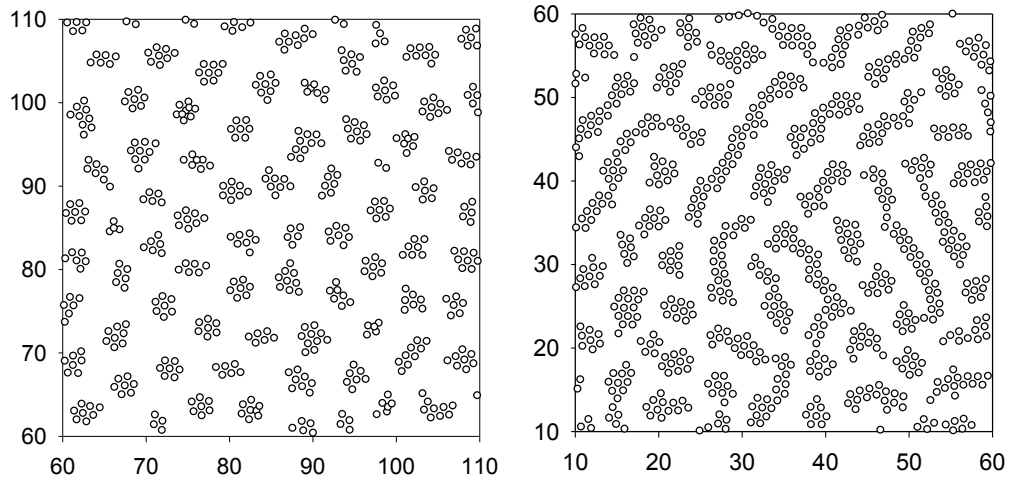

FIG. 1: A projection of a representative configuration of the particles adsorbed at the surface. Left: density $\rho_0 = 0.005$ and temperature $T^* = 0.13$, and the dimensionless wall-particle attraction $\gamma = 1.5$. Right: $\rho_0 = 0.00676$, $T = 0.15$, $\gamma = 2.5$.

A part of this work was done during **the secondment of M. Litniewski (IPC) to BSTU in Minsk and A. Ciach (IPC) to UNLP in La Plata**.

The results are published in: M. Litniewski and A. Ciach "Effect of aggregation on adsorption phenomena" J. Chem. Phys. **150**, 234702 (2019); https://doi.org/10.1063/1.5102157

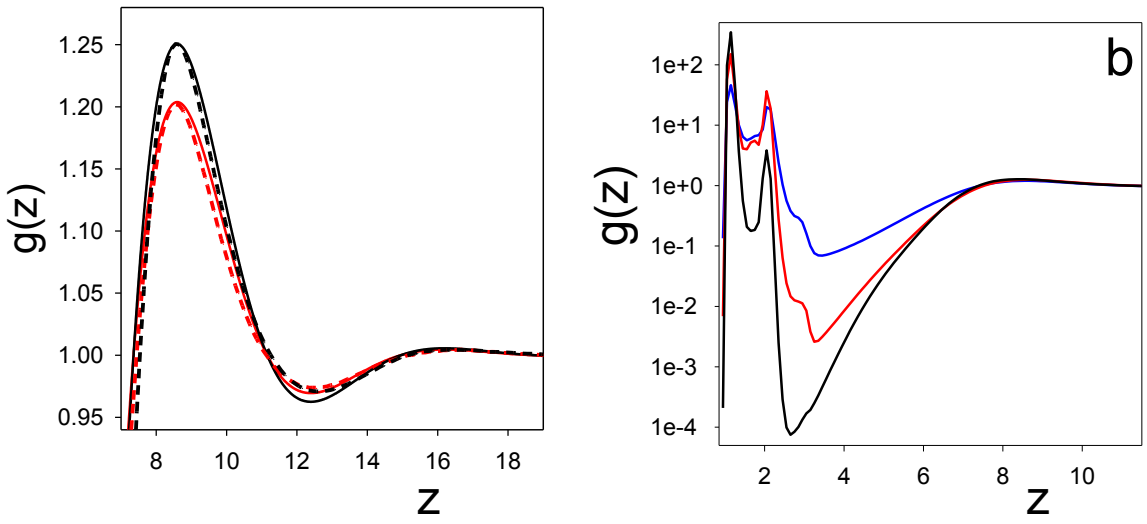

FIG. 2: The density profile in direction perpendicular to the wall for density $\rho_0 = 0.005$ and temperature $T^* = 0.13$. Left: large distances from the wall. The dotted lines are the simulation results, and the continuous lines are the best fits to Eq.(3). The red and black lines correspond to $\gamma = 0.5, 1.0$, respectively. Right: small distances from teh wall. From the bottom to the top lines (black, red, blue) $\gamma = 1.5, 1, 0.5$. z is in units of the particle diameter.

1.b. Adsorption anomalies in a 2D model of cluster-forming systems.

Adsorption on a boundary line confining a monolayer of particles self-assembling into clusters was studied by MC simulations. We focused on a system of particles interacting via the SALR potential for fixed chemical potential μ and temperature T. For such thermodynamic states, we computed the adsorption defined by the equation

$$\Gamma(\mu) = \int_0^\infty (\rho(z) - \rho_b) dz \tag{4}$$

where $\rho(z)$ and ρ_b are the average density at the distance z from the wall and in the bulk, respectively. The aim of our study was a determination of the effect of cluster formation on the amount of particles adsorbed at the confining wall.

We calculated the adsorption isotherms for a triangular lattice model with nearest-neighbor attraction $-J_1$ and third-neighbor repulsion JJ_1, introduced earlier in Refs.[1, 2]. In addition, we calculated structural characteristics such as the cluster-size distribution in the bulk and near the wall, density profile in direction perpendicular to the wall and the

correlation function in the layers parallel to the wall. We have found a close relation between the shape of the adsorption isotherm and the structure of the fluid.

We have found that $\Gamma(\mu^*)$ exhibits a maximum upon structural transition between structureless and disordered cluster fluid (Fig.3). The adsorption decreases for increasing chemical

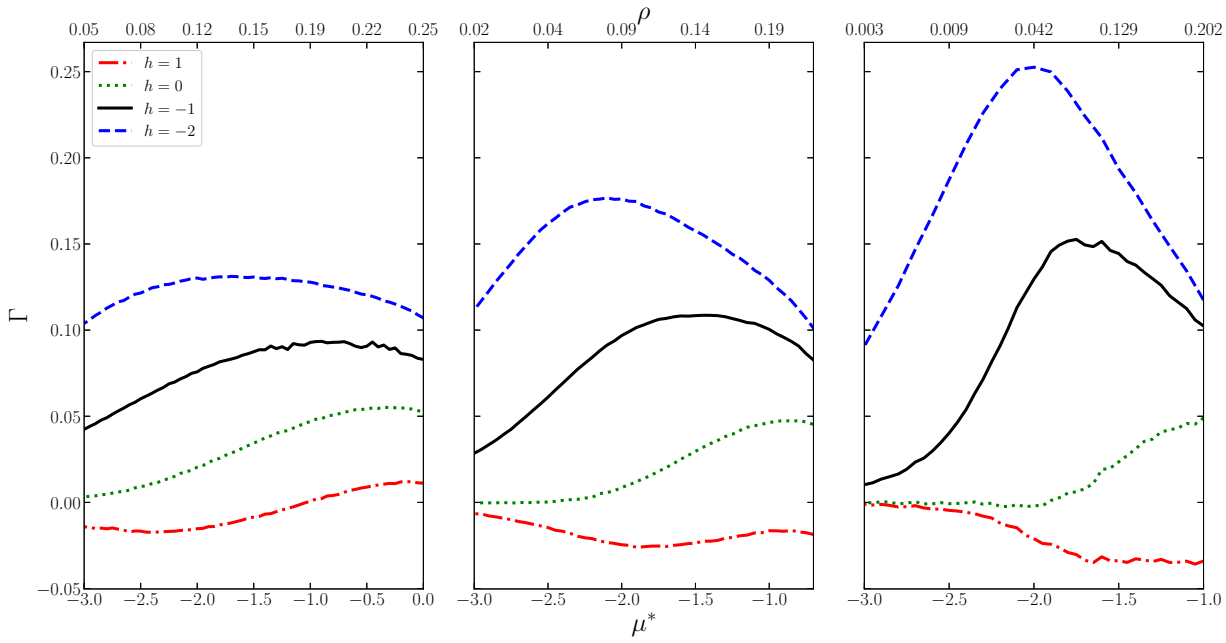

FIG. 3: Adsorption Γ *versus* the chemical potential μ^* for different values of the wall-particle interaction h at the system temperatures $T^{=}$1.0 left, $T^* = 0.7$ central and $T^* = 0.5$ right panels. Γ, $T^* = k_BT/J_1$ and $\mu^* = \mu/J_1$ are dimensionless.

potential when (i) clusters dominate over monomers in the bulk, (ii) the density profile in the direction perpendicular to the confining line exhibits an oscillatory decay, (iii) the correlation function in the layer near the adsorbing wall exhibits an oscillatory decay in the direction parallel to this wall. Our report indicates striking differences between simple and complex fluid adsorption processes.

A major part of this work was done during **the secondments of E. Bildanau and V. Vikhrenko from BSTU to IPC in Warsaw**.

The results are submitted for publication: E. Bildanau, J. Pękalski, V. Vikhrenko and A. Ciach, "Adsorption anomalies in a 2D model of cluster-forming systems", arXiv:1909.09374

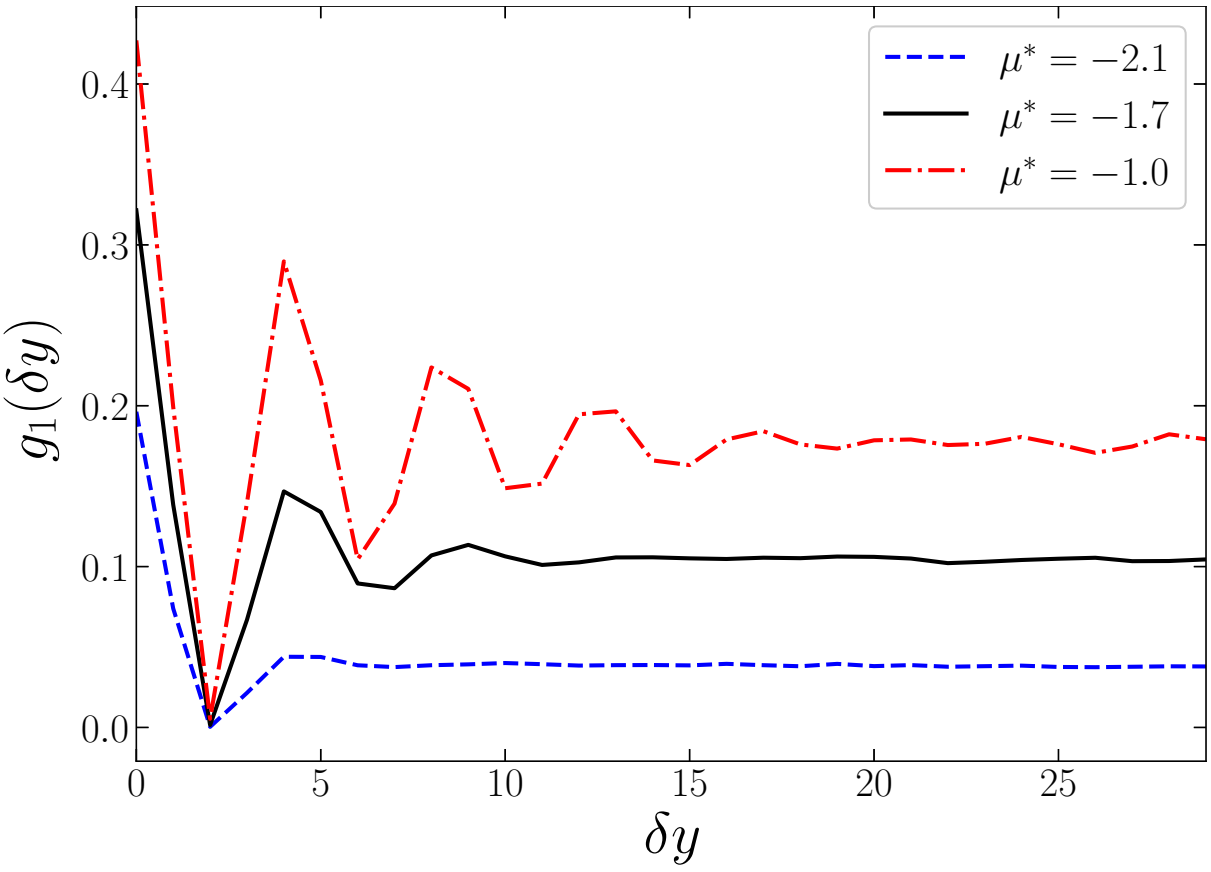

FIG. 4: Correlation functions $g_1(\delta y)$ along the wall for the first row for different values of the chemical potential, which correspond to the states before (dashed line), at (solid line) and after (dash-dotted line) the maximum of the adsorption $\Gamma(\mu^*)$ at temperature $T^* = 0.5$ and the particle-wall interaction energy $h = -1$.

1.c. Soft-particle fluid with competing interactions confined by a hard wall

A fluid interacting with a three-Yukawa (3Y) potential (Fig. 5) was studied in the bulk and in the vicinity of a hard wall. The amplitudes and the ranges of the respective Yukawa terms were chosen so as to reproduce the short-range attraction and long-range repulsion (SALR) between particles, thus offering a different model of a system with competing interactions. An interesting feature of this potential is the softness of the core, which describes the possibility of partial overlap between particles. The model can, therefore, describe effective pair interaction in a variety of soft matter systems such as star-polymer blends, dispersions of polymer-grafted nanoparticles, solutions of proteins, microgel suspensions etc.

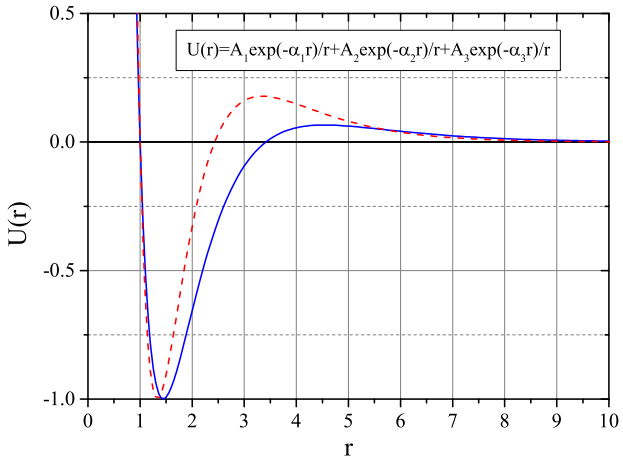

FIG. 5: Pair interaction potential used for calculations: solid blue line – Model M1; and red dashed line – Model M2).

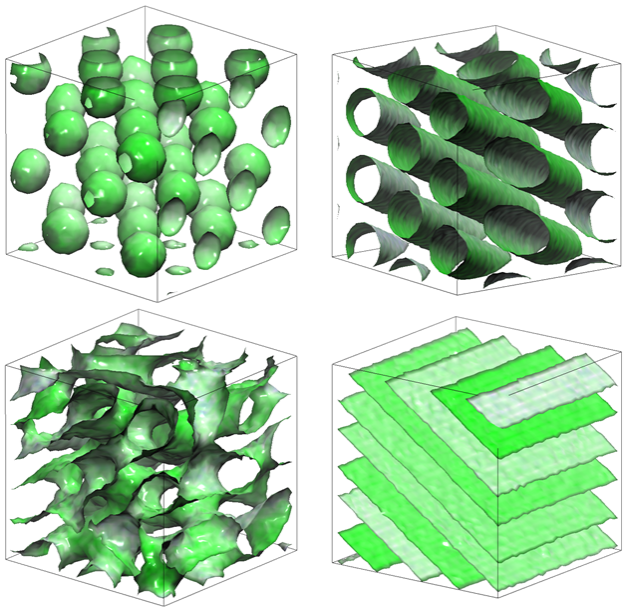

FIG. 6: Examples of mesoscopic structures observed from MD studies: BCC lattice of spherical clusters, cylinders, lamellas, and gyroids (clockwise starting from top left).

Two sets of parameter values for the three-Yukawa potential were considered to built the SALR type potential ("Model M1" and "Model M2" in Fig. 5). A series of Monte-Carlo (MC) computer simulations across a wide range of temperatures and densities were performed. The results showed that the model proposed can describe spontaneous appearance in the system of various mesostructures including lamellar and gyroidal phases, hexagonally packed

cylindrical phases, cubically ordered and disordered clusters formed by particles or voids (Fig. 6). Furthermore, we observed that these self-assembly effects become more pronounced when the fluid is confined between two inert walls, e.g. close to the walls cluster formation can occur at temperatures higher than those required for micro-segregation in the bulk. As the temperature increases, the clusters vanish, though distinct inhomogeneuity near the interface still persists.

A classical field theory was subsequently applied to describe the micro-structure and thermodynamics of a 3Y fluid at high temperatures and reproduce the density profiles obtained from our simulations. As a first step, we investigated the homogeneous phase in the bulk and close to a hard wall. For the bulk region, a bicubic equation for generalized screening parameters was derived and solved analytically. The solution of this equation was used to calculate the structure factor, the pressure, and the chemical potential. Based on these results, we studied the phase behavior by constructing the binodal curves and the lambda-lines. The critical value of the wave vector responsible for cluster formation was determined. Explicit analytical expressions for the radial distribution function were derived and compared to the MC data (Fig. 7).

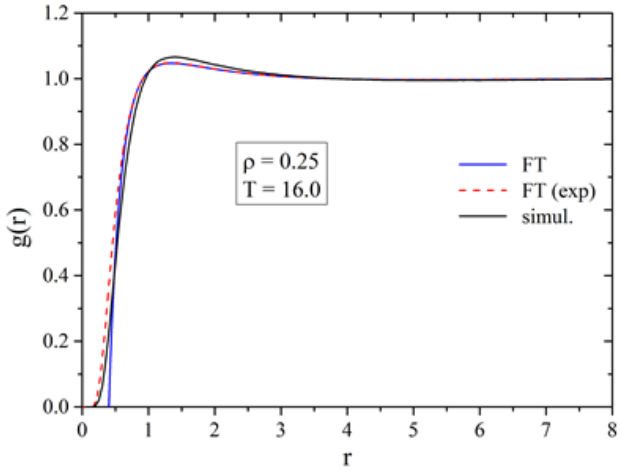

FIG. 7: Radial distribution function (Model M1). Theoretical calculations vs. MC simulations.

Next, we considered mean field description of a 3Y-fluid in the vicinity of a hard wall. An integral equation of the Euler-Lagrange type was obtained for the density profile. Linearization of this equation led to a system of second-order differential equations which were solved using the contact theorem as a boundary condition. The solution of these equations led to explicit analytical expressions for the density profile, which proved to be in very good

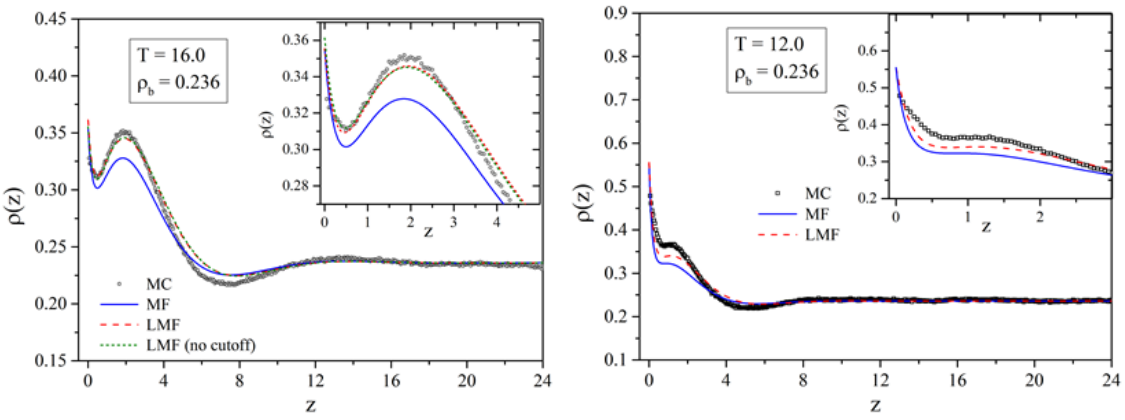

FIG. 8: Density profile for Model M1 (left panel) and Model M2 (right panel). Theoretical estimations vs MC simulations data.

agreement with the simulations data. These results are presented in Fig. 8 along with the numerical solution of the mean field equation. Close to the wall we observe an interesting split of the first maximum of the density profile. We relate the presence of this bilayer to the competing nature of the pair potential between particles, because this specific behavior had not been observed earlier in a simple attractive two-Yukawa fluid. The agreement between theoretical predictions for the profile and the MD simulations data improves with increasing temperature.

This work was done during the secondments to Minsk (BSTU) of T. Patsahan, I. Kravtsiv, M.Holovko (ICMP) and D. di Caprio (CPT) in year 2019. This work has been presented in the III CONIN workshop and in an conference:

1. I. Kravtsiv, T. Patsahan, D. di Caprio, M. Holovko. Soft-particle system with competing interactions: field theory treatment. III CONIN Workshop: Systems with competing electrostatic and short-range interactions. 1–2 July 2019, Lviv, Ukraine. Book of abstracts, p. 14 (oral)

2. I. Kravtsiv, M. Holovko, T. Patsahan and D. di Caprio. Soft-core fluid with competing interactions in contact with a hard wall. 5-th Conference "Statistical Physics: Modern Trends and Applications". July 3–6, 2019, Lviv, Ukraine. Book of abstracts, p. 131 (poster)

1.d. Adsorption of SALR particles on spherical surface.

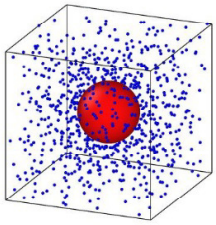

FIG. 9: Instantaneous configuration of a SALR system in the presence of a spherical surface.

In a previous work (Litniewski & Ciach, J. Chem. Phys. 150, 234702 (2019)) studied adsorption of SALR particles confined in a slit pore (two parallel flat surfaces), but in this study it is investigated adsorption on a spherical surface. A Monte Carlo simulation in the grand canonical ensemble is implemented to evaluate the equilibrium properties of this system. It consists in a 3D box (with periodical boundary conditions), with a nanosphere in the center of it (see Fig. 9). Particles into the box (blue ones) interact via a SALR potential, composed by a Lennard-Jones potential plus a repulsive Yukawa tail. A Lennard-Jones interaction between particles and the nanosphere is imposed. The objective is to evaluate how the curvature modify the cluster size distributions and shapes, density profiles from the center of the nanosphere, and the adsorbed mass near the nanosphere.

Work is in progress on these systems. **Part of this work was done during the secondment of Alina Ciach (IPC) in UNLP and during the seconment of Ariel Meyra (UNLP) to IPC. Guillermo Zarragoicoechea (UNLP) was also part of the team working on this topic.**

1.e. Mesoscopic theory for systems with competing interactions near a confining wall.

Mesoscopic theory for self-assembling systems near a planar confining surface has been developed. Euler-Lagrange (EL) equations and the boundary conditions (BC) for the local volume fraction and the correlation function were derived from the DFT expression for the grand thermodynamic potential. Various levels of approximation were considered for the obtained equations.

The lowest-order nontrivial approximation (GM) resembles the Landau-Brazovskii type

theory for a semiinfinite system. Unlike in the original phenomenological theory, however, all coefficients in our equations and BC are expressed in terms of the interaction potential and the thermodynamic state. The GM is based on the approximation for the competing interaction potential in Fourier representation

$$\hat{U}(k^2) = \hat{U}(k_0^2) + v(k^2 - k_0^2)^2 + ..., \tag{5}$$

where k is a wavenumber of a density wave, and $2\pi/k_0$ is the energetically favored length-scale of inhomogeneities. In GM, the average volume fraction $\zeta_b + \Delta\zeta_0(z)$ at the distance z from the wall satisfies the equation

$$\beta\Big(v\frac{\partial^4}{\partial z^4} + 2vk_0^2\frac{\partial^2}{\partial z^2} + vk_0^4 + \hat{U}(k_0^2)\Big)\Delta\zeta_0(z) + g^{(1)}(\zeta_b, \Delta\zeta_0(z)) = 0. \tag{6}$$

The correlation function in Fourier represention in the direction parallel to the wall and in real-space representation in the perpendicular direction, $\tilde{G}(k_\parallel|z_1, z_2)$, satisfies the equation

$$\beta\left[v\frac{\partial^4}{\partial z_1^4} + 2v(k_0^2 - k_\parallel^2)\frac{\partial^2}{\partial z_1^2} + d(z_1, k_\parallel)\right]\tilde{G}(k_\parallel|z_1, z_2) = \delta(z_1 - z_2) \tag{7}$$

where ζ_b is the volume-fraction in the bulk, $d(z_1, k_\parallel) = \hat{U}(k_0^2) + v(k_\parallel^2 - k_0^2)^2 + k_BTg^{(2)}(\zeta_b, \Delta\zeta_0(z_1))$, and $g^{(n)}(\zeta_b, \Delta\zeta_0(z))$ are functions depending on the assumed approximation for the free-energy of the hard-sphere reference system.

Analytical solutions of the linearized equations (6) and (7),

$$\Delta\zeta_0(z) = \mathcal{A}e^{-\alpha_0 z}\cos(\alpha_1 z + \vartheta) \tag{8}$$

and

$$\begin{aligned}\tilde{G}(k_\parallel|z_1, z_2) = {} & \mathcal{A}_-(k_\parallel)e^{-\alpha_0(k_\parallel)|z_1 - z_2|}\cos[\alpha_1(k_\parallel)|z_1 - z_2| + \theta_-(k_\parallel)] \\ & + \mathcal{A}_+(k_\parallel)e^{-\alpha_0(k_\parallel)(z_1 + z_2)}\cos\left[\alpha_1(k_\parallel)(z_1 + z_2) + \theta_+(k_\parallel)\right],\end{aligned} \tag{9}$$

show exponentially damped oscillations of the volume fraction and the correlation function in the direction perpendicular to the confining surface. The inverse lengths, $\alpha_{0,1}(k_\parallel)$, depend strongly on $k_\parallel$. Only the longitudinal waves with large wavelengths in the planes at different z are correlated. The correlations show oscillatory decay in directions parallel to the confining surface too, with the decay length increasing significantly when the system boundary is approached.

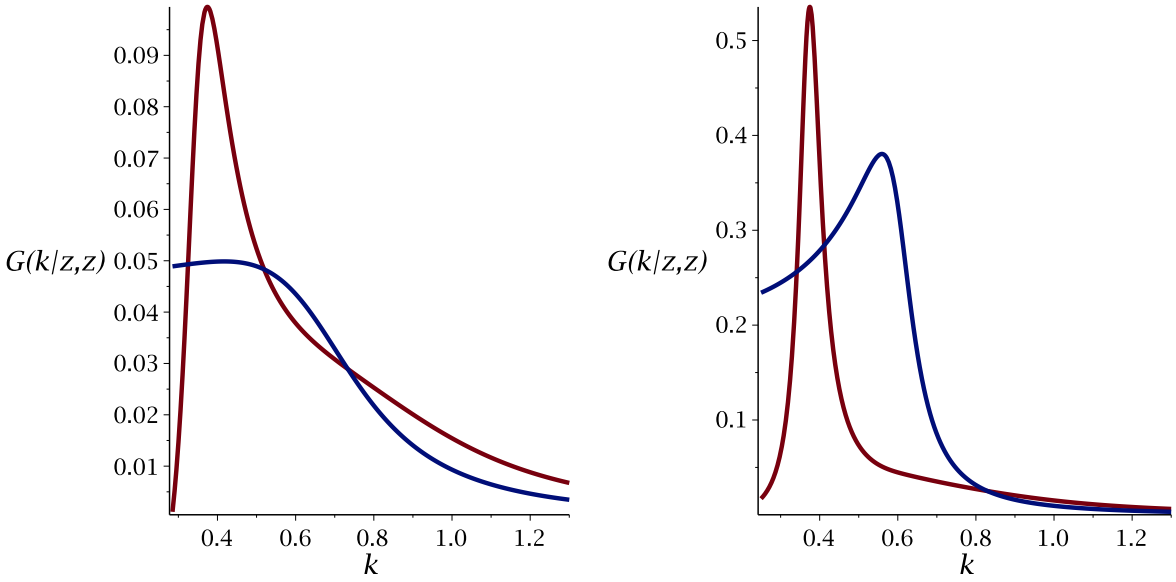

FIG. 10: The correlation function (9) in 2D Fourier representation in the planes parallel to the wall at $z = 0$ (upper line), and $z = \infty$ (lower line) for the Percus-Yevick reference system and the interaction potential (10) with $K_1 = 1, K_2 = 0.2, \kappa_1 = 1, \kappa_2 = 0.5$. The thermodynamic state corresponds to high temperature/low density (left) and low temperature/medium density (right). The wavenumber is in units of inverse particle diameter.

As a particular example of competing interactions, the double-Yukawa potential

$$V(r) = -\frac{K_1}{r}e^{-\kappa_1 r} + \frac{K_2}{r}e^{-\kappa_2 r}. \tag{10}$$

has been considered. The correlation function in the mixed representation is shown in Fig.10 for weak (left panel) and strong (right panel) inhomogeneities in the bulk. Since the decay length is the larger the narrower is the peak, we can see much larger correlation length close th the wall than far from it.

Our results agree with simulations on a qualitative level. The framework of our theory allows for a systematic improvement of the accuracy of the results.

A part of this work was done during **the secondment of A. Ciach (from IPC) to UNLP in La Plata**.

The results are submitted for publication: A.Ciach, "Mesoscopic theory for systems with competing interactions near a confining wall", arXiv:1910.04474

1.f. Microscopic theory for non-homogeneous systems with competing interactions.

At a first stage of this research, a two-level statistical theory of inhomogeneous condensed matter was developed. It naturally combines the two main approaches of statistical physics, the method of correlation functions and the method of thermodynamic functionals of the density field. This made it possible, from a single point of view, to describe the thermodynamic and structural properties of homogeneous and inhomogeneous systems, including nanoscale systems, and also to consider the contributions of thermodynamic fluctuations when calculating thermodynamic potentials for fluid systems. The influence of various kinds of defects can be taken into account when studying deformed crystalline systems including nanostructured materials with their unique properties. The idea of a reduced description in the theory of fluctuations based on a statistical expression for the effective Hamiltonian of an inhomogeneous system (in the sense of Landau-Lifshitz) is exploited.

The two-level statistical mechanical theory of inhomogeneous fluctuating systems is used to construct a phase diagram of a simple system, study surface phenomena in heterogeneous (macroscopic and nanoscale) systems with flat and spherical interfaces, describe the adsorption phenomenon on various substrates, and also for statistical mechanical study of the crystal lattice relaxation at the interface with another coexisting phase (macroscopic) or at the interface of nanoparticles of different sizes.

Based on the method developed, an equation is obtained for the radial discrete profile of the filling numbers of elementary cells of the conditional distributions method, which determine the local concentration of particles in the vicinity of any of the cells whose centers form coordination spheres l = 1, 2, ..., L for the face-centered cubic (fcc) lattice [2]. A method for the numerical calculation of the unary and binary distribution functions of atoms or molecules in the vicinity of the lattice sites has been developed. With their help, the radial displacements of the nodes of the deformed fcc lattice and the standard deviations of atoms (molecules) from new sites of nanoparticles of different sizes (L=16) have been calculated at several temperatures below the triple point temperature for a simple molecular macroscopic system.

The two-level statistical method developed for molecular systems is generalized to describe the structure and thermodynamic characteristics of colloidal systems with competing SALR (Short-range Attraction Long-range Repulsion) interaction. As an example, the vari-

ation of the free energy of the system with SALR interparticle interactions (short range Lennard-Jones plus long range repulsive Yukawa) as a function of the wave number is shown in Fig. 11. The variation of the Gibbs thermodynamic potential attains minimum at the wave number that corresponds to the wavelength 28.5σ (χ=$0.22/\sigma$, σ is the spatial parameter of Lennard-Jones potential) at ρ=0.8, while at ρ=0.9 the minimum corresponds to the homogeneous state (χ=0). This means that the inhomogeneous state with periodic variation of the density is stable at ρ=0.8. The thermodynamic region of inhomogeneous states is shown in Fig. 12.

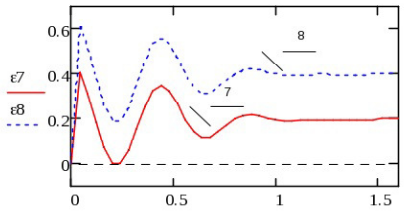

FIG. 11: The variation of the Gibbs thermodynamic potential ϵ7, ϵ8 versus the wave number χ at the reduced temperature θ=5 and average concentration c =0.8 (7) and 0.9 (8) (in units of the Lennard-Jones parameters).

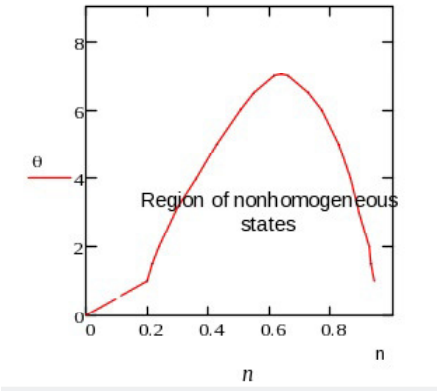

FIG. 12: The coexistence line between homogeneous and nonhomogeneous states on the temperaturedensity thermodynamic plane.

A part of this work has been performed by I. Narkevich (BSTU) during his secondment to ICMP and disseminated in two research articles:

- I.Narkevich, Two-level statistical mechanical method for describing inhomogeneous systems. Part 1. LAP Lambert AP, Mauritius, 2019 (In Russian).

- I.Narkevich, Statistical justification of Brazovskiis prediction of the transition of a colloidal solution from a homogeneous to inhomogeneous state. Proceedings of the Belarusian State Technological University. 2019. Ser. 3, No. 2. P. 2833. (In Russian).

2. Core-shell particles self-assembling on an interface between coexisting fluid phases.

A triangular lattice model for self-assembly of hard-core soft-shell particles on an interface between coexisting fluid phases has been introduced and studied. We assumed that the particles interact with short-range repulsion long-range attraction (SRLA) effective potential. Monte Carlo simulations and analytical calculations of thermodynamic and structural peculiarities of nanoparticles were performed.

In the first step we studied the effect of the range and shape of effective interactions that follow from different properties of the soft shell of the particles and different properties of the interface. The ground states of the system with the nearest neighbor repulsion and third neighbor attraction are of a hexagonal order at concentrations 1/4, 3/4 and 1, while at the concentration 1/2 stripes of particles are formed. On the other hand, the systems with nearest neighbor repulsion and second or fifth neighbor attraction have similar hexagonally ordered ground states at lattice concentrations $1/3, 2/3, 1$, in addition to the vacuum state. However, if in the system with nearest neighbor repulsion J_1 and fifth neighbor attraction $-J_5$ the repulsion of the second neighbors J_2 is added, the ground states become very complex (Figs. 13 and 14). The critical value of the ratio of the interaction constants between the first and second neighbors, J_1/J_2 that separates different successions of the ground states is equal to 3. For $J_1/J_2 < 3$ the ground states for concentrations $3/9 \leq c \leq 6/9$ are degenerated. Apart from determining the ground states for different interactions and chemical potential of the particles, we have started Monte Carlo simulations of thermodynamic and structural peculiarities of nanoparticles at different temperatures. The work is in progress.

A substantial part of this work was done during **the secondment of Vera Hryshina, Vyacheslav Vikhrenko and Yaroslav Groda from BSTU to IPC in Warsaw**.

The results are published in: Ya.G.Groda, V.S.Hryshina, A. Ciach and V.S.Vikhrenko, "Phase diagram of the lattice fluid with SRLA potential on the plane triangular lattice",

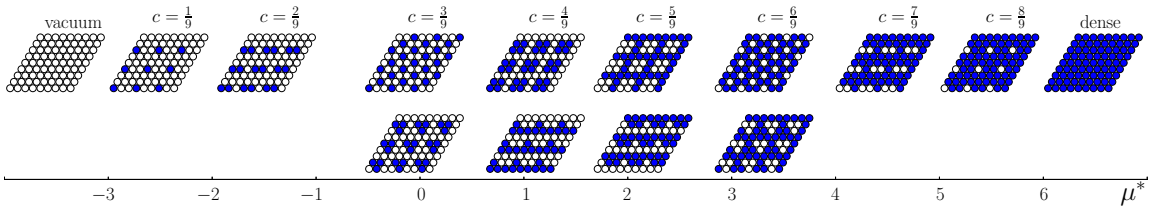

FIG. 13: The ground states of the system with nearest and second neighbor repulsion and fifth neighbor attraction at the ratio of the interaction constants $J_1/J_2 = 2$.

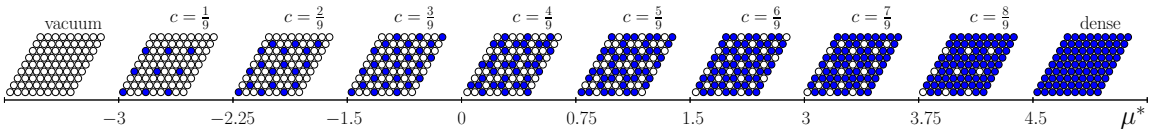

FIG. 14: The ground states of the system with nearest and second neighbor repulsion and fifth neighbor attraction at the ratio of the interaction constants $J_1/J_2 = 4$.

Journal of the Belarusian State University. Physics. 2019. No. 3. P. 8191. Publication. DOI:https://doi.org/10.33581/2520-2243-2019-3-81-91. (In Russian)

3. Simulation studies of the SALR systems under confinement.

3.a. SALR confined in pipes with different cross sections.

Last year we studied the behaviour of SALR molecules under cylindrical confinement at thermodynamic conditions at which the hexagonal cylindrical phase is the stable phase in bulk. We found that cylindrical confinement promotes the formation of helical structures whose morphology depends both on the pore radius and boundary conditions.

Now we have extended this study to confining channels of different cross-section, including elliptical, triangular, squared and hexagonal geometries. As before, we focus on thermodynamic conditions at which the hexagonal cylindrical phase is stable in bulk. Our results show that the structure of the confined fluid depends on the commensurability of the bulk periodic structure with the confining cross-section of the channel. It was also found that narrow wedges favour the formation of straight cylinders. This explains why the cylindrical phase often remains stable in triangular channels, whereas in hexagonal channels the

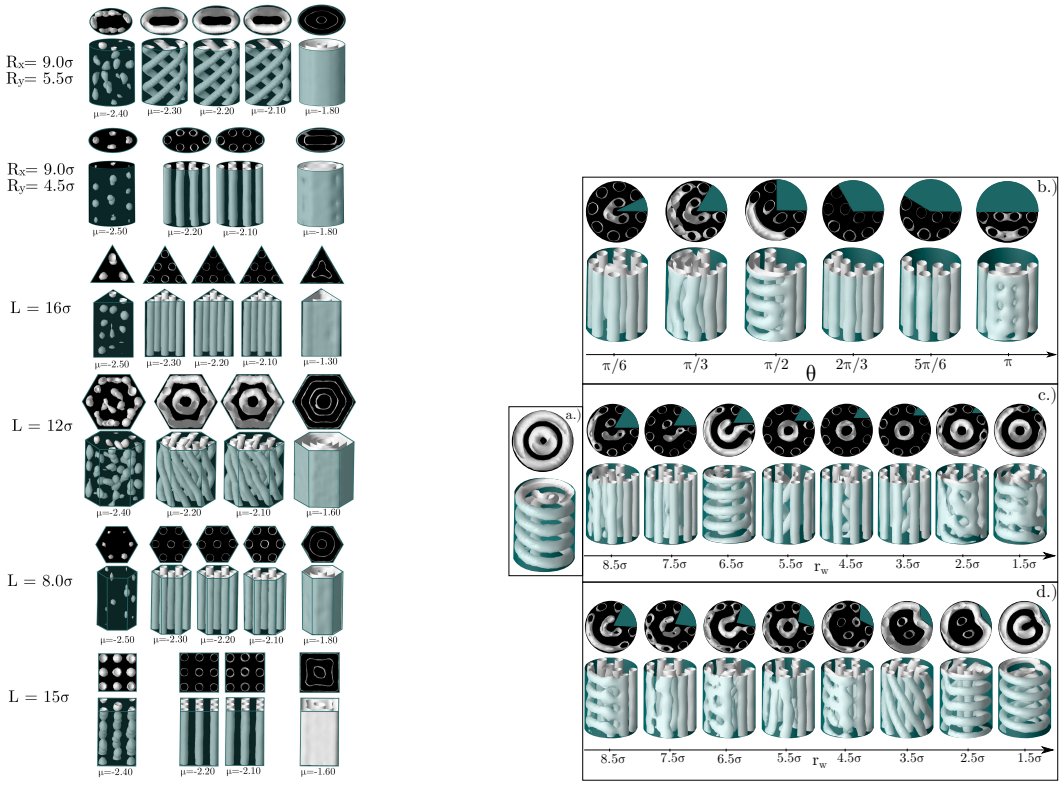

FIG. 15: Left figure: Structure of confined SALR in channels of different shapes at different values of chemical potential μ. Right figure: a) Original helical structure, and b) c) d) structure of the confined fluid when wedges of different size and shape are inserted in the pore cavity.

confined fluid organizes either into straight channels or helical structures depending on the pore size. It also explains the higher tendency of the confined fluid to form straight cylinders in elliptical channels of larger eccentricity. Finally we have also found that the structure of the confined fluid can be tuned by inserting wedges within the confining pore.

In summary, our work shows that the structure of the confined fluid can be finely tuned by modifying the cross-section size and geometry of the confining pore, but also inserting wedges that favour the formation of straight cylinders. **This investigation has been performed at IPC (H. Serna and W.T. Góźdź) in collaboration with CSIC (E. Noya). Ariel Meyra (UNLP) contributed to discussions during his secondment to IPC.** It is summarized in the article "The influence of confiement on the structure of colloidal systems with competing interactions" by Horacio Serna, Eva G. Noya and W.T. Góźdź, that has just been accepted for publication in Soft Matter.

3.b Confinement on spherical shells

We have investigated the behavior of different cluster phases in a spherical shell where the shell width is comparable to the width of the colloidal clusters. We performed Monte Carlo simulations in the grand canonical ensemble, i.e., at fixed chemical potential, temperature and volume (μ, V, T).

As in the previous study we used the square-well-linear potential, whose bulk phase diagram has been recently evaluated in Ref. 3.

We investigate the behavior of the colloidal clusters confined in a spherical shell. Particles are confined into a spherical shell of the thickness 6σ, with its external radius R_o and internal radius R_i. R_o is defined as the distance from the center of the sphere to the point where the external potential is infinite. A simulation starts with few molecules randomly distributed into the shell. 3-5 10^6 MC steps are used for equilibration and 1 10^6 steps for productions. Here, a Monte Carlo step is a trial move of the all N molecules and an addition or deletion trial is attempt at each step.

In Fig 16 we present the results of our calculations for two different values of the chemical potential μ. At theses values of μ in bulk we obtain cluster crystals and hexagonally arranged cylindrical crystals. We have examined how these phases are deformed in confined spherical shells. As shown in Fig 16b the cylindrical clusters confined in a spherical shape are arranged in in such way to maximize the length of the cluster. In the case of the spherical clusters we observe that they are uniformly distributed on in a spherical shell, see Fig. 16.

(a) 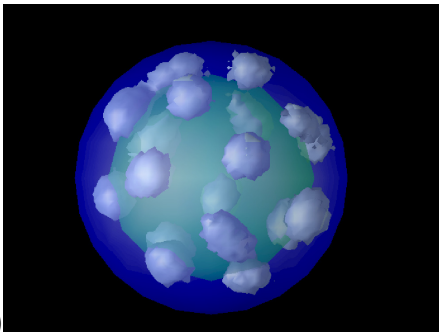 (b) 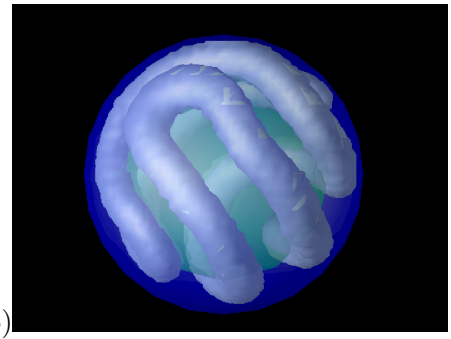

FIG. 16: The local density plots for a shell with the radius $R_o = 10\sigma$ for two different chemical potentials; (a) $\mu = -2.60$, (b) $\mu = -2,325$. The surface represent the local density with the value $\rho(\mathbf{r}) = 0.4$.

Part of this work was done during **the secondment of Ariel Meyra (UNLP) to IPC and during secondment of Wojciech Góźdź (IPC) to UNLP.**

---

4. Hyperuniformity in systems with competing interactions

During 2019, the work developed between CSIC and UNLP focused along two main lines, that are intertwined in WP1 and WP2. The systems studied are characterized by clustering due to the presence of long range repulsive forces (mostly Coulomb either in 2D/3D or dipolar-like) and interactions that can be cast into the class of charged systems.

4.a. Hyperuniformity and structure of dipolar fluids on curved surfaces. Systems constrained in curved systems are ubiquitous in nature (water-air interfaces, cell membranes, etc ...), and we have investigated ways to determine whether the structure of patterns on these curved systems can be characterized as hyperuniform and disordered. This work is bio-inspired by the hyperuniform character found in the space distribution of photoreceptors in avian retina (itself a curved surface). Our studies carried out with regular and random patterns together with patterns formed by particles interacting with long-range interactions, show that a regular non-hyperuniform pattern is described by a number variance following

$$\sigma_n^2(a) = \langle\rho\rangle s(a), \tag{11}$$

where $s(a)$ is the sampling area (a being the radius of the base of the spherical segment with one base used as sampling element) and $\langle\rho\rangle$ is the average density. This linear dependence with the sampling area is similar to the one found in Euclidean spaces. Similarly, we have found that systems for which

$$\frac{\sigma_n^2(a)}{s(a)} \to 0. \tag{12}$$

the patterns display structural hyperuniformity. In practice this translates for the series of systems studied by us a series of scaling relations with the base radius a as shown in the table I, where we consider parallel dipoles (with a repulsion scaled with a parameter α), interactions charge-dipole and charge-charge, for particles on spherical surfaces of radii 15

TABLE I: Summary of the scaling behavior of the number variance with the geometric parameters of the sampling window for uncorrelated, regular point patterns, and fluid configurations on the sphere. In the latter instance, results for two different radii are presented.

Point pattern	scaling
Poisson distribution	$\sigma_n^2(a) \propto s = (1-\sqrt{1-(a/R)^2})2\pi R^2$
Uniform distribution	$\sigma_n^2(a) \propto a^2 = s(1-s/(4\pi R^2))/\pi$
Triangular lattice	$\sigma_n^2(a) \propto a$
Fibonacci lattice	$\sigma_n^2(a) \propto a$
$R = 15$	
LJ fluid	$\sigma_n^2(a) \propto a^2$
$U_{dd}(\alpha = 1)$	$\sigma_n^2(a) \propto a^2$
$U_{dd\|\|}(\alpha = 1)$ fluid	$\sigma_n^2(a) \propto a^{1.8}$
U_{dc} $(\gamma = 1)$ fluid	$\sigma_n^2(a) \propto a^{1.7}$
U_{cc} $(\beta = 1)$ fluid	$\sigma_n^2(a) \propto a^{1.4}$
$R = 5$	
$U_{dd\|\|}(\alpha = 1)$ fluid	$\sigma_n^2(a) \propto a^{1.7}$
$U_{dd\|\|}(\alpha = 3)$ fluid	$\sigma_n^2(a) \propto a^{1.3}$
$U_{dd\|\|}(\alpha = 6)$ fluid	$\sigma_n^2(a) \propto a^{1.1}$

and 5 (in particle diameter units). The quadratic scaling of the non-hyperuniform systems contrasts with the linearly approaching scaling that systems with long range repulsive iinteractions. Some hyperuniform configurations corresponding to the parallel dipole-dipole (α/r^3) interactions are shown in Figure 17.

Interestingly, this spherical patterns have been shown to correspond to optimal Quasi Monte Carlo (QMC) integration schemes. These have been extensively used to construct efficient quadratures to evaluate illumination integrals which are essential in the rendering of photorealistic images. This connection between hyperuniformity and rendering, can actually explain why disordered hyperuniformity is the structure of choice when it comes do design an optimal photoreceptor distribution in birds. This is directly connected with the next point to be discussed in this report. **Part of this work was performed during the secondments of Ariel Meyra and Guillermo Zarragoicoechea (UNLP) to CSIC.**

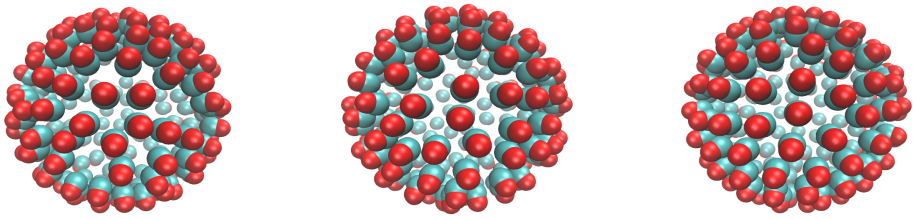

(a) $\alpha = 1.0$ (b) $\alpha = 3.0$ (c) $\alpha = 6.0$

FIG. 17: Illustration of simulated systems for representative states of different repulsion strength when the long-range interaction is $U_{dd||}$ corresponding to hyperuniform patterns.

All the results concerning this line of research have been published in Article Meyra, A. G.; Zarragoicoechea, G. J.; Maltz, A. L.; Lomba, E. & Torquato, S. *Hyperuniformity on spherical surfaces*, Phys. Rev. E, 2019 , **100** , 022107.

4.b. Extension to other curved surfaces.

We are studying the behaviour of dipolar or Yukawa particles embedded on the surface of revolution generated from a Cassini oval. The study is focused on hyperuniformity and structural properties. Cassini oval is defined in 2D in two center bipolar coordinates as d1 d2=b2 or in a quadratic polynomial Cartesian equation:

$$[(x-a)^2 + y^2)][(x+a)^2 + y^2)] = b^4 \tag{13}$$

Details of parameters can be seen in the Figure 18.

After some manipulation it is possible to write an expression in polar coordinates defining the oval (being θ the angle measured from $z+$):

$$r = [-a^2 cos(2\theta) + (b^4 - a^4 + a^4 cos^2(2\theta))^{1/2}]^{1/2} \tag{14}$$

Depending on the relationship of parameters, it is possible to obtain a variety of revolution objects, from spherical surfaces to red blood cell shapes (see Figure19).

In red blood cell like surfaces, for instance, we will be able to obtain fluctuation on particle number in function of the area, the euclidean radius defining that area, or its perimeter. For

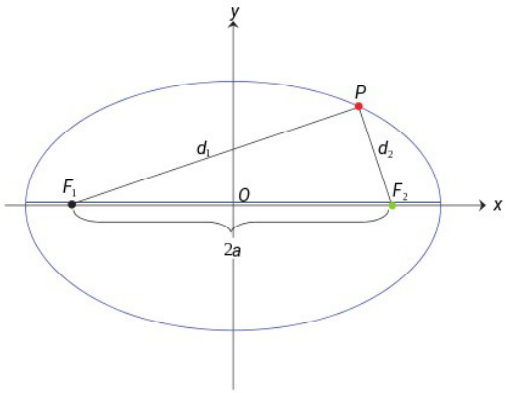

FIG. 18: Illustration of the parameters used to define a Cassini oval.

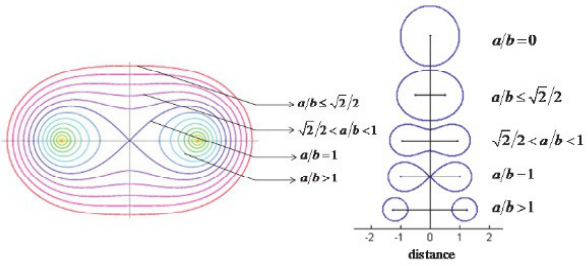

FIG. 19: Dependende of the geometry on the relation between the a and b parameters

doing that we have algorithms to calculate euclidean distances over curved surfaces, based on tessellation of the surface. A typical snapshot for a system of 900 dipolar particles at

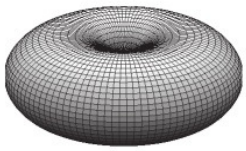

FIG. 20: Tesselation of a curved surface.

T*=1.3, on a surface with $a/b = 2^{1/2}/2$ is shown In Figure 21.

Simulations are in progress on these systems. **Part of this work was developed during the secondments of Ariel Meyra and Guillermo Zarragoicoechea (UNLP) to CSIC, and during the secondment of Enrique Lomba (CSIC) to UNLP.**

Part of the work mentioned above has been presented in poster session at StatPhys27.

Hyperuniformity on curved surfaces. Guillermo J. Zarragoicoechea, Ariel G. Meyra,

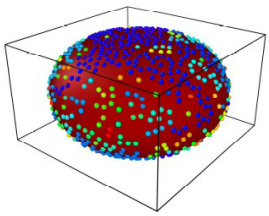

FIG. 21: Instantaneous configuration of dipolar particles on a Cassimi oval.

Enrique Lomba Garca, Salvatore Torquato. 27th International Conference on Statistical Physics, StatPhys 27, of the International Union of Pure and Applied Physics (IUPAP), July 8-12 2019, Buenos Aires, Argentina.

4.c. A minimal model for avian retina.

An example of biological system where clustering plays a key role in the distribution of photoreceptors in bird retina. As mentioned before, the special structure can be understood as an optimum way for mapping a three-dimensional representations of an image onto a two-dimensional one, which implies the calculation of certain surface integrals. This is accomplished thanks to a the presence of disordered hyperuniformity in the distribution of each and every photoreceptor pattern (of the five types present in birds). Interestingly, the simplest solution which would be a regular hexagonal pattern (which is the perfect limit of hyperuniformity) as done in arthropods is not possible in birds, since contrary to insects with faceted eyes, photoreceptors are polydisperse, in size and number, which prevents the formation of regular (crystal-like) patterns. In our work, we have proposed a minimal statistical mechanical model (three receptor types, rgb) which can mimic the behavior of avian retina. To that aim we have first investigated the nature of the interactions between particles that can lead to multi-hyperuniformity, i.e. the anomalous suppression of long range density and concentration fluctuations. We now that long range potentials whose Fourier transform fulfills $\lim_{Q\to} \beta\tilde{u}_{ij}(Q) \propto Q^{-\alpha}$ with $\alpha > 0$ can in principle be hyperuniform in the disordered phase. From an analysis of the Ornstein-Zernike equation, we have found that

$$\lim_{Q\to 0} \beta\tilde{u}_{ii}(Q) \;\propto\; Q^{-\alpha} \tag{15}$$

$$\lim_{Q\to 0} |\tilde{\mathbf{u}}(Q)| \neq 0 \tag{16}$$

where $|\ldots|$ is the determinant of the matrix formed with the Fourier transformed species-species interactions. In practice, this can be shown to be fulfilled if the Lorentz-Berthelot mixing rules are not satisfied in the limit $Q \to 0$, namely

$$\lim_{Q\to 0} \left(\tilde{u}_{ij}(Q)^2 - \tilde{u}_{ii}(Q)\tilde{u}_{jj}(Q)\right) \neq 0 \tag{17}$$

In our work we have experimented with a system with long range interaction of 2D Coulombic nature, which qualitatively lead to structure factors similar to those found in bird photoreceptors.

$$\beta u_{\alpha\beta}(r) = \begin{cases} \infty & \text{if } r < (1+\Delta(1-\delta_{\alpha\beta}))\sigma \\ -\Gamma_{\alpha\beta}\log r/\sigma & \text{if } r \geq (1+\Delta(1-\delta_{\alpha\beta}))\sigma \end{cases} \tag{18}$$

where $\Gamma_{\alpha\beta}$ is a coupling parameter, σ the hard core exclusion diameter between like species, and $\Delta < 0$ is the negative non-additivity parameter. We have considered $\Delta = -2$ in order to guarantee local heterogeneity, i.e. to avoid clustering of the same species of photoreceptors. In Figure 22 we can see a snapshot in which one can clearly see how the different types of photoreceptors tend to cluster together. The structure factor is found to fulfill the require

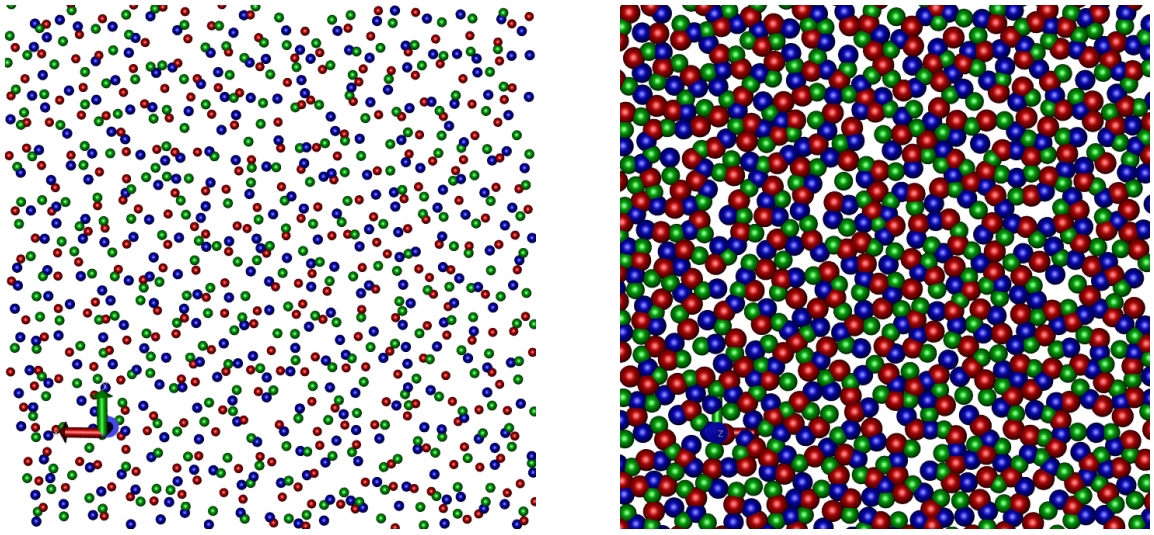

(a)$\rho\sigma^2 = 0.2$ (b)$\rho\sigma^2 = 0.8$

FIG. 22: Snapshots of Monte Carlo configurations of the three component symmetric NAHD plasma for $\gamma = 5$ and $\Delta = -2$.

conditions $\lim_{Q\to 0} S_{ii}(Q) = 0$ for all three photoreceptor types and looks qualitatively similar

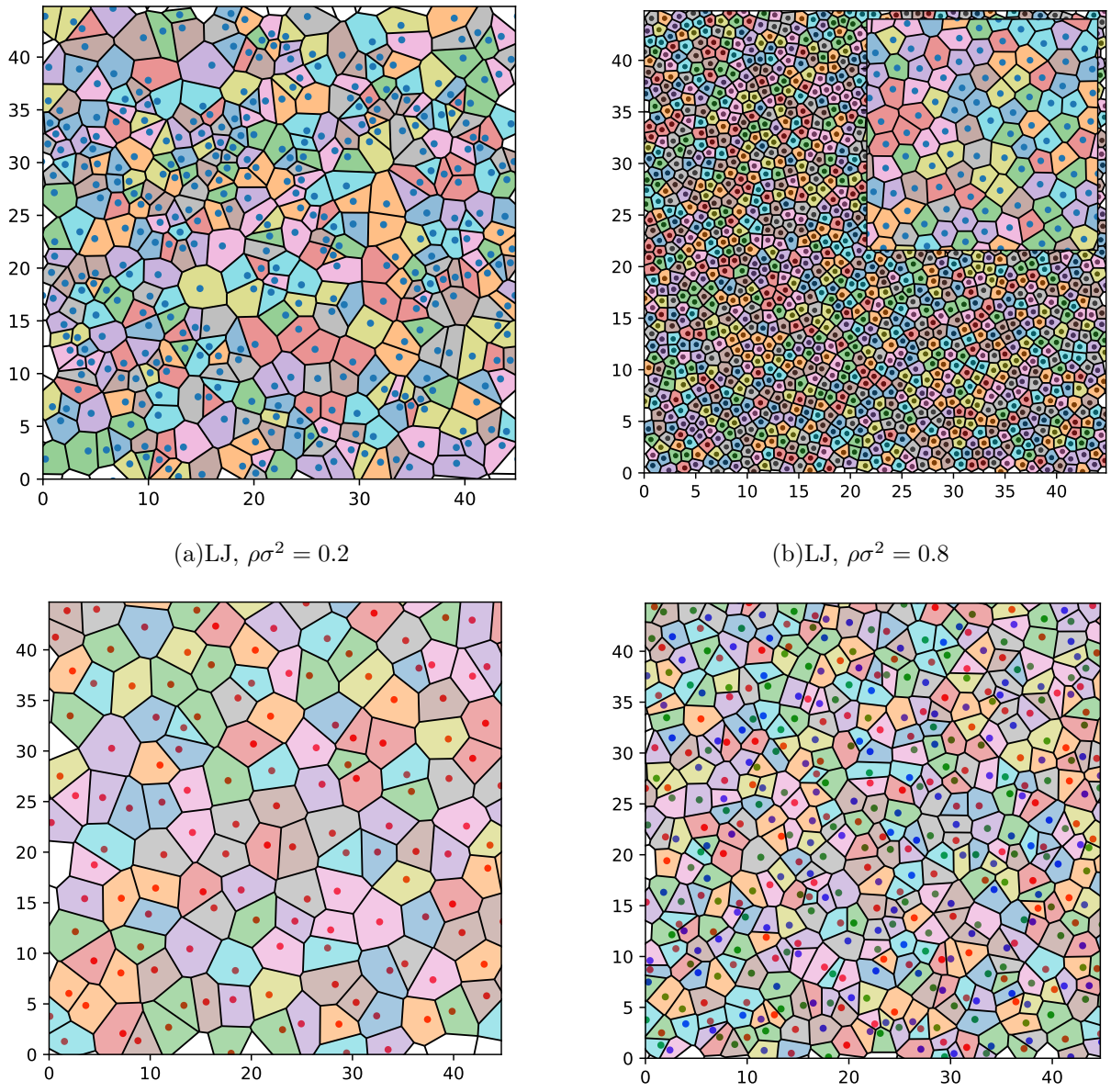

(a)LJ, $\rho\sigma^2 = 0.2$

(b)LJ, $\rho\sigma^2 = 0.8$

(c)NAHD plasma, $\rho_{red}\sigma^2 = 0.2/3$

(d)NAHD plasma, $\rho\sigma^2 = 0.2$

FIG. 23: (a) and (b) Voronoi tessellations corresponding to a LJ fluid configuration for $\rho\sigma^2 = 0.2$ and $\rho\sigma^2 = 0.8$, and $k_BT/\epsilon = 2$. The inset on the right figure is a zoom of the central area of the simulation cell. The low density LJ configuration yields a Voronoi tessellation indistinguishable from that of a random configuration of points.(c) and (d) represent tessellations for our non-additive hard disk plasma model for avian retina

to the experimental one. More interestingly, if one looks at the area so to speak "assigned" to each photoreceptor, we find a Voronoi tessellation very symmetric with respect to the regular one, as can be qualitatively appreciated in figure 23 where the tessellation for the

photoreceptor distribution (non-additive hard-disk plasma) is compared to tessellations for two-dimensional Lennard-Jones fluids.

A quantitative analysis of this tessellations shows that hyperuniform patterns lead to symmetric Gaussian area distributions centered around the lattice pattern, whereas non-hyperuniform patterns lead to asymmetric log-normal or Γ-distributions. In summary, one could say that disordered hyperuniformity corresponds to nature's way of reproducing crystal-like properties when crystallization itself is frustrated by factors such as size and number polydispersity. **Part of this work was developed during the secondments of Leandro Guisández (UNLP) at CSIC and IPC.** These results are about to be sent to publication, in E. Lomba, J.J. Weis, L. Guisndez, and S. Torquato, *A minimal statistical-mechanical model for multihyperuniform patterns in avian retina*, (to be submitted, 2019).

DISSEMINATION AND PUBLICATION ACTIVITIES

Activity 1.

M. Litniewski and A. Ciach, "Effect of aggregation on adsorption phenomena, J. Chem. Phys. **150**, 234702 (2019), publication.

Activity 2.

J. Pękalski, E. Bildanau and A. Ciach, "Self-assembly of spiral patterns in confined system with competing interactions", Soft Matter, **15**, 7715 (2019), publication.

Activity 3.

E. Bildanau, J. Pękalski, V. Vikhrenko and A. Ciach, "Adsorption anomalies in a 2D model of cluster-forming systems", Phys. Rev. E (accepted), arXiv:1909.09374, publication.

Activity 4.

A.Ciach, "Mesoscopic theory for systems with competing interactions near a confining wall", submitted, arXiv:1910.04474, publication.

Activity 5.

Horacio Serna, Eva G. Noya and W.T. Góźdź, "Assembly of helical structures in systems with competing interactions under cylindrical confinement", Langmuir **35**, 702-708 (2018), publication.

Activity 6.

Horacio Serna, Eva G. Noya and W.T. Góźdź, "The influence of confinement on the structure of colloidal systems with competing interactions", Soft Matter (accepted), publication.

Activity 7.

Ariel G. Meyra, Guillermo J. Zarragoicoechea, Alberto. L. Maltz, Enrique Lomba and Salvatore Torquato, "Hyperuniformity on spherical surfaces" Phys. Rev. E **100**, 022107 (2019), publication.

Activity 8.

Enrique Lomba, J.J. Weis, Leandro Guizandez, and Salvatore Torquato, "A minimal statistical-mechanical model for multihyperuniform patterns in acain retina" to be submitted, publication.

Activity 9.

Ya.G.Groda, V.S.Hryshina, A. Ciach and V.S.Vikhrenko, "Phase diagram of the lattice fluid with SRLA potential on the plane triangular lattice", Journal of the Belarusian State University. Physics. 2019. No. 3. P. 8191. DOI:https://doi.org/10.33581/2520-2243-2019-3-81-91. (In Russian), publication.

Activity 10.

Groda Ya.G., Vikhrenko V.S., di Caprio D., "Lattice fluid with attractive interaction between nearest neighbors and repulsive interaction between next-next-nearest neighbors on simple cubic lattice", Journal of the Belarusian State University. Physics. 2019; 2: 84 95, https://doi.org/10.33581/2520-2243-2019-2-84-95 (in Russian), publication.

Activity 11.

I.Narkevich, Two-level statistical mechanical method for describing inhomogeneous systems. Part 1. LAP Lambert AP, Mauritius, 2019 (In Russian).

Activity 12.

I.Narkevich, Statistical justification of Brazovskiis prediction of the transition of a colloidal solution from a homogeneous to inhomogeneous state. Proceedings of the Belarusian State Technological University. 2019. Ser. 3, No. 2. P. 2833. (In Russian).

Activity 13.

Alina Ciach, Theory for Systems with Spontaneous Inhomogeneities on a Mesoscopic Length Scale, XXII International Conference on Chemical Thermodynamics in Russia, Petersburg, 19-23.06.2019, plenary lecture.

Activity 14.

Alina Ciach, "Density Functional Theory for Systems with Competing Interactions", 5-th Conference on Statistical Physics: Modern Trends and Applications July 3-6, 2019 Lviv, Ukraine, invited lecture.

Activity 15.

Ya.G.Groda, D.di.Caprio, A. Ciach, V.S.Vikhrenko, Equilibrium properties of three-dimensional lattice fluids with SALR interactions. III CONIN Workshop: Systems with competing electrostatic and short-range interactions 12 July 2019, Lviv, Ukraine. Book of Abstracts. P. 13. (Lecture).

Activity 16.

J. Pękalski, Structural transitions in closed systems with competing interactions, III CONIN workshop: "Systems with competing electrostatic and short-range interactions July, 1-2 2019, Lviv 2019, Ukraine, lecture.

Activity 17.

Alina Ciach, "Density Functional Theory for Systems with Competing Interactions", The 5th International Soft Matter Conference (ISMC2019), Edinburgh, United Kingdom, 3-7 June 2019, poster.

Activity 18.

H. Serna, E.G. Noya and W.T. Góźdź , "Effects of confinement on self-assembly in systems with competing interactions", The 5th International Soft Matter Conference (ISMC2019), Edinburgh, United Kingdom, 3-7 June 2019, poster.

Activity 19.

M. Litniewski and A. Ciach, "Effect of aggregation on adsorption phenomena, 5-th Conference on Statistical Physics: Modern Trends and Applications July 3-6, 2019 Lviv, Ukraine, poster.

Activity 20.

V.S.Hryshina, A. Ciach, J. Pekalski, V.S.Vikhrenko, "Ground state of a system with SRLA interaction". III CONIN Workshop: Systems with competing electrostatic and short-range interactions 12 July 2019, Lviv, Ukraine. Book of Abstracts. P. 20. (Poster)

Activity 21.

V.S.Vikhrenko, Ya.G.Groda, D.di.Caprio, "Thermodynamic and Structural Properties of Systems with SALR Interaction on Two- and Three-dimensional Lattices". The 5-th Conference Statistical Physics: Modern Trends and Applications Programme and Abstracts 36 July 2019, Lviv, Ukraine. P. 168. (Poster)

Activity 22.

I. Kravtsiv, T. Patsahan, D. di Caprio, M. Holovko. "Soft-particle system with competing interactions: field theory treatment". III CONIN Workshop: Systems with competing electrostatic and short-range interactions. 1–2 July 2019, Lviv, Ukraine. Book of abstracts, p. 14 (Oral).

Activity 23.

I. Kravtsiv, M. Holovko, T. Patsahan and D. di Caprio. Soft-core fluid with competing interactions in contact with a hard wall. 5-th Conference "Statistical Physics: Modern Trends and Applications". July 3–6, 2019, Lviv, Ukraine. Book of abstracts, p. 131 (Poster).

Activity 24.

Guillermo J. Zarragoicoechea, Ariel G. Meyra, Enrique Lomba Garca, Salvatore Torquato. "Hyperuniformity on curved surfaces" 27th International Conference on Statistical Physics, StatPhys 27, of the International Union of Pure and Applied Physics (IUPAP), July 8-12 2019, Buenos Aires, Argentina.

---

[1] J. Pękalski, A. Ciach, and N. G. Almarza, *J. Chem. Phys.* **140**, 114701 (2014).

[2] N. G. Almarza, J. Pękalski, and A. Ciach, *J. Chem. Phys.* **140**, 164708 (2014).

[3] Zhuang, Y.; Zhang, K.; Charbonneau, P. Equilibrium Phase Behavior of a Continuous-Space Microphase Former. *Physical Review Letters* **116**, 098301 (2016).